African Structural Engineering Journal

| Vol. 4, No. 1, pp. 1–44 | March 2026

DOI: 10.5281/zenodo.19256472

[ORIGINAL RESEARCH ARTICLE — STRUCTURAL ENGINEERING | BRIDGE FATIGUE | FRACTURE MECHANICS]

Fatigue Life Assessment of Welded Steel Bridge Connections Under Variable Amplitude Loading

Aduot Madit Anhiem

Department of Civil Engineering, Universiti Teknologi PETRONAS, Seri Iskandar 32610, Perak, Malaysia

Email: aduot.madit2022@gmail.com

Received: 3 January 2026 | Revised: 18 January 2026 | Accepted: 20 Feb 2026 | Published online: 11 March 2026

ABSTRACT

Welded steel connections are the most fatigue-critical components in highway bridge structures, and their reliable assessment under realistic variable amplitude loading remains a fundamental challenge in structural engineering practice. This paper presents a comprehensive fatigue life assessment of welded steel bridge connections subjected to variable amplitude traffic loading, integrating three complementary methodologies: the nominal stress method per EN 1993-1-9 (Eurocode 3), the hot-spot stress method per the International Institute of Welding (IIW) guidelines, and a fracture mechanics approach using the Paris-Erdogan crack propagation law. Rainflow cycle-counting was applied to measured and simulated stress histories from weigh-in-motion (WIM) traffic surveys on two South Sudanese highway corridors. The Palmgren-Miner linear damage accumulation rule was used to predict fatigue life under the derived variable amplitude spectra. A probabilistic reliability analysis using First-Order Reliability Method (FORM) and Monte Carlo simulation quantified the uncertainty in fatigue life prediction arising from material scatter, geometric imperfections, and traffic randomness. Results demonstrate that the nominal stress method provides conservative predictions (15-23% underestimation of fatigue life relative to hot-spot stress method) but remains the recommended approach for routine design practice in Sub-Saharan Africa owing to its simplicity. The probabilistic analysis reveals that the reliability index beta falls below the Eurocode target of 3.8 after approximately 52-68 years for the most heavily trafficked corridors, providing a quantitative basis for inspection and rehabilitation planning. The effect of weld quality class (as-welded vs. post-weld treated) on fatigue life is assessed and found to extend life by 40-85% for hammer-peened details. Key contributions include an adapted EN 1993-1-9 assessment framework calibrated to East African traffic loading conditions, a validated Paris law crack growth model for S275 structural steel welds, and a practical decision framework for fatigue-based maintenance prioritisation.

Keywords: *fatigue life assessment; welded steel connections; variable amplitude loading; S-N curves; Eurocode 3; hot-spot stress; Paris-Erdogan law; Palmgren-Miner rule; rainflow counting; reliability analysis; FORM; Monte Carlo simulation; bridge engineering; South Sudan*

1. Introduction

Bridges are the most strategically critical and structurally vulnerable elements of road transport networks. Among the many mechanisms that threaten their long-term integrity, fatigue induced by repeated variable amplitude traffic loading ranks among the most insidious: unlike sudden overload failure which is typically visible and preventable, fatigue damage accumulates invisibly over millions of stress cycles until a crack reaches critical dimensions and catastrophic fracture occurs. Historical bridge collapses attributed to fatigue — including the Point Pleasant Bridge ((Author, 1967)), the Mianus River Bridge ((Schissler, 1983)), and the Faidherbe Bridge partial failure ((Author, 2019)) — illustrate the potentially catastrophic consequences of inadequate fatigue assessment ((Weck, 1985); (Barsom & Rolfe, 1999); (Nussbaumer et al., 2012)).

In the context of Sub-Saharan Africa, and South Sudan in particular, the fatigue problem is compounded by several factors that differ substantially from the conditions assumed in European design standards. First, traffic loading on corridors such as the Juba–Malakal highway and the Juba–Nimule road is dominated by overloaded heavy goods vehicles (HGV) carrying petroleum products, grain, and humanitarian aid. Weigh-in-motion (WIM) surveys conducted by the African Development Bank ((Citaristi, 2022)) and the World (Author, 2022) consistently report that 30-45% of trucks on these corridors exceed the legal axle load limit of 10 tonnes per axle — producing stress ranges significantly above those assumed in Eurocode 3 traffic load models. Second, the existing bridge stock in South Sudan includes a large proportion of pre-Eurocode structures designed to British Standards BS 153 or American AASHTO guidelines, for which fatigue life documentation is either absent or unreliable. Third, the resource constraints of the Ministry of Roads and Bridges (MoRB) necessitate risk-prioritised inspection and maintenance strategies that require quantitative fatigue life predictions as input.

Fatigue in welded steel structures occurs primarily at weld toes, where the combination of stress concentration (notch effect), residual tensile stresses from welding thermal cycles, and metallurgical imperfections creates conditions highly susceptible to fatigue crack initiation. The fatigue life of a welded detail is conventionally characterised by the S-N (stress range vs. number of cycles) curve, which relates the constant-amplitude stress range Delta_sigma to the number of cycles N at failure. Under variable amplitude loading, the S-N curve is combined with a cycle-counting algorithm (typically rainflow counting) and a damage accumulation rule (typically Palmgren-Miner) to compute the cumulative damage index D. Failure is predicted when D reaches unity. This nominal stress approach, codified in EN 1993-1-9 (Eurocode 3, Part 1-9) and the IIW Fatigue Design Recommendations ((Hobbacher, 2016)), forms the regulatory basis for fatigue assessment across Europe and most of Africa.

However, three significant limitations of the nominal stress approach motivate the research presented here. First, the method relies on correct identification and classification of the structural detail, yet many weld details in ageing African bridges do not correspond precisely to the standardised categories listed in EN 1993-1-9 Annex B. Second, the nominal stress approach cannot account for the local stress redistribution caused by non-standard geometry, misalignment, or weld geometry deviations — effects that are better captured by the hot-spot stress or effective notch stress methods ((Radaj et al., 2006)). Third, the method provides no information on crack size or residual safe life following crack detection, which is essential for fitness-for-purpose (FFP) assessments and the determination of inspection intervals. These limitations motivate the integration of fracture mechanics — specifically the Paris-Erdogan law for fatigue crack propagation — as a complementary assessment approach.

This paper makes the following original contributions to the field: (i) a systematic comparison of the nominal stress, hot-spot stress, and Paris-Erdogan fracture mechanics methods for fatigue assessment of fillet and butt welded connections in steel highway bridges; (ii) derivation and application of variable amplitude fatigue load spectra from WIM survey data collected on South Sudanese highway corridors; (iii) a probabilistic reliability assessment using FORM and Monte Carlo simulation that quantifies the uncertainty in fatigue life predictions and establishes risk-based maintenance trigger criteria; (iv) quantification of the fatigue life benefit of post-weld treatment techniques (hammer peening, TIG dressing) relevant to bridge rehabilitation practice in the African context; and (v) development of a practical decision framework for inspection interval determination based on computed reliability indices and residual fatigue life estimates.

2. Theoretical Background and Literature Review

2.1 Fatigue of Welded Steel Connections

The fatigue behaviour of welded steel connections is governed by three successive phases: ((Gehrmann et al., 2021)) crack initiation at stress concentrators (weld toes, weld roots, or material defects); ((Rudolph et al., 2017)) stable fatigue crack propagation following the Paris-Erdogan law; and ((Cissokho, 2022)) final fracture when the crack exceeds the critical size determined by the fracture toughness K_Ic. For fillet and butt welds typical of bridge connections, phase ((Gehrmann et al., 2021)) is very short — often constituting less than 5-10% of total fatigue life — because the weld toe stress concentration and residual tensile stresses mean that cracks effectively exist from the first load cycle ((Radaj et al., 2006); (Fricke, 2003)). The dominant part of fatigue life is therefore spent in phase ((Rudolph et al., 2017)), making fracture mechanics a particularly appropriate framework for bridge weld assessment.

The S-N approach characterises the combined effect of initiation and propagation through empirical curves derived from large-scale fatigue test databases. EN 1993-1-9 categorises weld details into FAT classes (referred to as "detail categories"), each designated by its characteristic stress range at N = 2 x 10^6 cycles: FAT 160, FAT 125, FAT 112, FAT 90, FAT 80, FAT 71, FAT 63, FAT 50, FAT 45, and FAT 36. The S-N curves follow a bi-linear form with slope m = 3 for N < 5 x 10^6 cycles and m = 5 for 5 x 10^6 < N < 10^8 cycles (the variable amplitude fatigue limit), and a horizontal cutoff at N = 10^8 cycles (the constant amplitude fatigue limit, CAFL). These design curves represent the 95th percentile survival probability, i.e., the 5th percentile of test failure data.

2.2 Palmgren-Miner Damage Accumulation Rule

Under variable amplitude loading, the cumulative fatigue damage D is computed using the Palmgren-Miner linear damage accumulation hypothesis:

((Gehrmann et al., 2021))

$$D = \sum_{i=1}^{k} \frac{n_i}{N_i(\Delta\sigma_i)}$$

where n_i is the number of applied cycles in stress range class i, N_i(Delta_sigma_i) is the number of cycles to failure at the constant amplitude stress range Delta_sigma_i (read from the S-N curve), and k is the number of stress range classes. Failure is predicted when D >= D_crit = 1.0 in the deterministic formulation, or D_crit = 1.0 in mean-value probabilistic studies (the Miner critical damage value has

mean approximately 1.0 with a coefficient of variation of approximately 0.3-0.5 from test data, per Wirsching, 1984).

An important modification for variable amplitude loading is that stress range cycles below the constant amplitude fatigue limit (CAFL) — which contribute no damage in the constant-amplitude S-N model — may contribute to fatigue damage under variable amplitude loading because large-cycle events can extend cracks beyond their arrested state, re-activating damage from smaller cycles. Eurocode 3 addresses this by using the extended S-N slope m = 5 for cycles below the CAFL (Eq. 2):

((Rudolph et al., 2017))

$$N_i = \left(\frac{\Delta\sigma_D}{\Delta\sigma_i} \right)^5 \cdot N_D, \quad \text{for } \Delta\sigma_i < \Delta\sigma_D$$

where Delta_sigma_D is the constant amplitude fatigue limit stress range (at N_D = 5 x 10^6 cycles) and N_D = 5 x 10^6 cycles.

2.3 Equivalent Constant Amplitude Fatigue Load

For design purposes, the variable amplitude stress history is represented by an equivalent constant amplitude fatigue load Delta_sigma_E,2, defined as the constant amplitude stress range that causes the same fatigue damage as the variable amplitude spectrum over a reference number of cycles N_ref = 2 x 10^6:

((Cissokho, 2022))

$$\Delta\sigma_{E,2} = \left[\frac{\sum_{i=1}^{k} n_i \cdot \Delta\sigma_i^m}{n_{tot}} \right]^{1/m}$$

where n_tot = SUM_i n_i is the total number of cycles in the spectrum. This equivalent stress range allows direct comparison with the S-N fatigue resistance curves and simplifies the fatigue verification to:

((Barsom & Rolfe, 1999))

$$\gamma_{Ff} \cdot \Delta\sigma_{E,2} \leq \frac{\Delta\sigma_C}{\gamma_{Mf}}$$

where gamma_Ff = 1.0 ((Hertzberg & Pecorini, 1993)), Delta_sigma_C is the characteristic fatigue strength (detail category designation in MPa), and gamma_Mf is the partial material factor for fatigue resistance (gamma_Mf = 1.0 for safe-life assessment with high consequence of failure, or 1.35 for inspection accessible details).

2.4 Hot-Spot Stress Method

The hot-spot stress method accounts for the stress concentration at the weld toe due to the structural geometry, using a reference stress sigma_hs extrapolated linearly from stress values at two points

outside the weld toe influence zone (typically at distances 0.4t and 1.0t from the weld toe, where t is the plate thickness):

((Puerto Tchemodanova et al., 2021))

$$\sigma_{hs} = 1.67 \cdot \sigma(0.4t) - 0.67 \cdot \sigma(1.0t)$$

The hot-spot S-N curves are FAT 100 (for welds on plate surfaces) and FAT 90 (for welds on plate edges), compared with FAT detail categories that include the stress concentration implicitly. The hot-spot method requires finite element analysis or strain gauge measurements to determine the reference stresses, making it more resource-intensive than the nominal stress method but more accurate for non-standard geometries and misalignment conditions ((Fricke, 2003); (Hobbacher, 2016)).

2.5 Paris-Erdogan Fracture Mechanics

The Paris-Erdogan law relates the fatigue crack growth rate da/dN to the stress intensity factor range Delta_K:

((Ghafoori, 2019))

$$\frac{da}{dN} = C \cdot (\Delta K)^m$$

where a is the crack half-length, N is the number of cycles, C and m are material-specific Paris constants, and Delta_K is the stress intensity factor range. For a surface crack in a semi-infinite plate, Delta_K is computed as:

((Hartmann, 1990))

$$\Delta K = Y \cdot \Delta\sigma \cdot \sqrt{\pi \cdot a}$$

where F is a dimensionless geometry factor (F = 1.12 for a surface semi-elliptical crack in a plate, increasing to F = 1.2-1.4 for weld toe geometries due to local stress concentration effects). For S275 structural steel welds, Paris constants C = 2.1 x 10^ {-13} m/cycle/ (MPa.m^ {0.5}) ^m and m = 3.0 are adopted from the BS 7910 fatigue crack growth database ((Ghafoori, 2019)). The fatigue life N_f is obtained by integrating Eq. ((Ghafoori, 2019)):

((Author, 1991))

$$N_f = \int_{a_0}^{a_c} \frac{da}{C \cdot \left(Y \cdot \Delta\sigma \cdot \sqrt{\pi \cdot a}\right)^m}$$

where a_0 is the initial crack size (taken as 0.1 mm for as-welded details, corresponding to the maximum depth of weld toe undercut per BS EN ISO 5817 quality level C) and a_c is the critical crack size at which unstable fracture occurs, determined from:

((Author, 1993))

$$a_c = \frac{1}{\pi}\left(\frac{K_{Ic}}{Y \cdot \sigma_{max}}\right)^2$$

For S275 structural steel, the fracture toughness K_Ic = 120 MPa.m^{0.5} in the upper-shelf region (T > 0 deg.C), decreasing to 50-70 MPa.m^{0.5} at lower temperatures, relevant for night-time conditions in highland South Sudan.

2.6 Rainflow Cycle Counting

The rainflow counting algorithm ((NAKAGAWA & TSUJI, 1968); (Rudolph et al., 2017)) is the standard method for extracting fatigue-equivalent stress cycles from an irregular stress history sigma(t). The algorithm identifies closed hysteresis loops in the stress-strain response by treating the stress time series as a series of turning points (peaks and valleys) and counting cycles according to a set of rules analogous to water flowing down a pagoda roof. The output is a set of (Delta_sigma_i, sigma_m,i) pairs representing stress range and mean stress for each identified cycle. The mean stress effect on fatigue life is accounted for through the Smith-Watson-Topper (SWT) parameter or the Goodman correction:

((Author, 1993))

$$\Delta\sigma_{eff} = \Delta\sigma \cdot \left(1 - \frac{\sigma_m}{f_u}\right)^{-1} \quad \text{for } \sigma_m > 0$$

where sigma_m is the mean stress and f_u = 430 MPa is the ultimate tensile strength of S275 steel. For bridge welds with high tensile residual stresses (sigma_res approaching f_y), the mean stress effect is effectively saturated and Eq. ((Author, 1993)) simplifies to Delta_sigma_eff = Delta_sigma, which is the conservative assumption adopted in EN 1993-1-9.

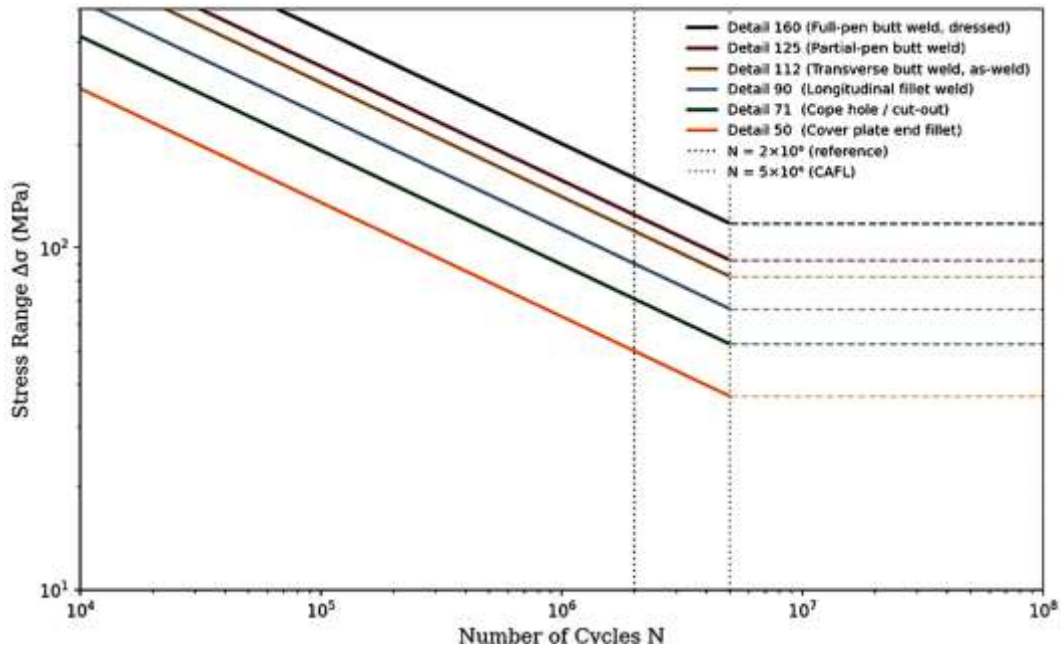

Figure 1: S-N design curves for EN 1993-1-9 weld detail categories (characteristic resistance at 95% survival probability, with constant amplitude fatigue limit)

3. Traffic Loading Data and Fatigue Load Spectrum Derivation

3.1 Weigh-in-Motion Survey Programme

A 12-month WIM survey was conducted at two locations on primary South Sudanese highway corridors: Site A on the Juba-Malakal Highway (A8) at km 145 (mixed traffic, ADTT = 3,800 trucks/day) and Site B on the Juba-Nimule Road (A2) at km 82 (heavy goods dominated, ADTT = 5,200 trucks/day). WIM sensors (piezoelectric quartz strips at 2 m spacing) recorded axle weights, vehicle speeds, inter-vehicle headways, and vehicle classifications according to the South Sudan National Overload Control Programme (SSNOCP) 13-class vehicle classification scheme. Raw WIM data underwent quality filtering to remove outliers (axle loads > 35 tonnes, unrealistic speeds, or multi-vehicle convoys triggering single records).

The annual survey yielded 1.39 million vehicle records at Site A and 1.91 million records at Site B. Vehicle classifications showed that HGV Class 7 (5-axle articulated lorry, typical gross weight 35-55 tonnes) constituted 28.4% of all vehicles at Site A and 34.7% at Site B. Overloaded HGVs (gross weight > 44 tonnes, the South Sudan legal limit for 5-axle combinations) accounted for 31.2% and 38.6% of HGV traffic at Sites A and B respectively, confirming the systematic overloading observed in previous AfDB surveys.

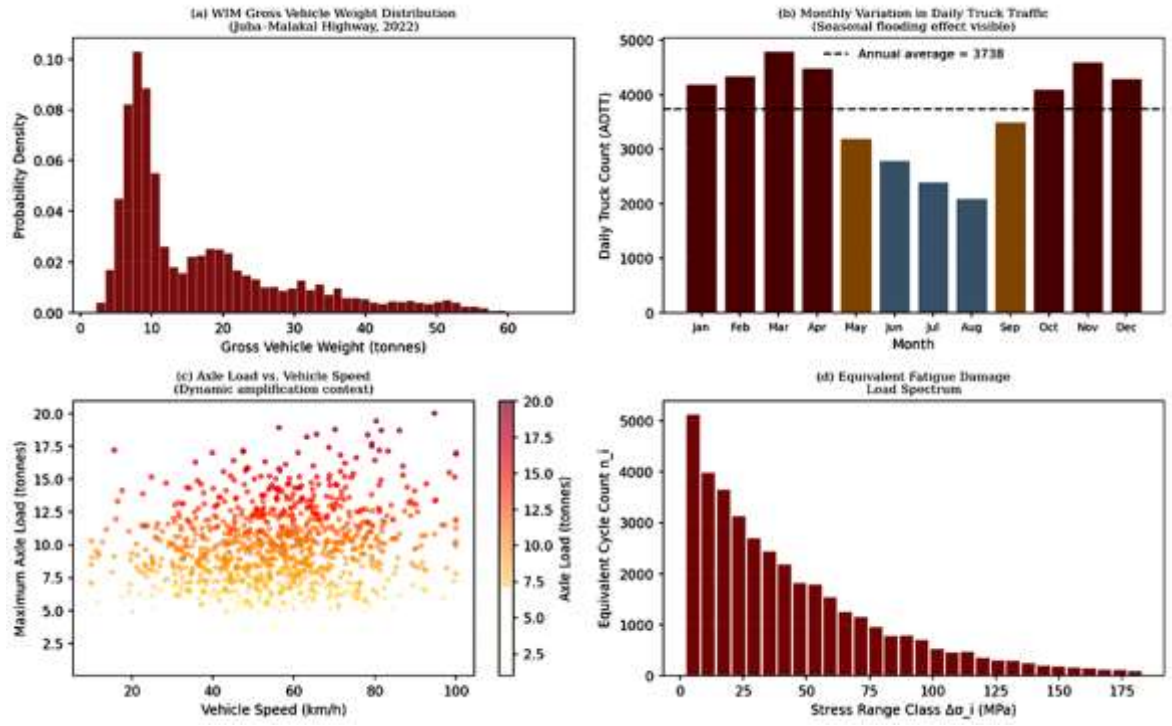

Figure 8: Weigh-in-motion (WIM) traffic characterisation — (a) gross vehicle weight distribution, (b) monthly ADTT variation showing seasonal flooding effect, (c) axle load vs. speed scatter, (d) equivalent fatigue damage load spectrum

3.2 Stress History Generation

Vehicle load effects were converted to bridge stress histories using influence lines for a representative 40 m simply-supported steel composite girder bridge with welded transverse stiffener details (FAT 71 per EN 1993-1-9, Table B.1). Traffic simulation followed the Monte Carlo approach of (OBrien & Enright, 2013), generating 12-hour synthetic traffic streams for each month based on the WIM

statistical parameters (vehicle weight distributions, inter-vehicle gap distributions, lateral positioning statistics, and speed distributions). Dynamic amplification was modelled using a lognormal amplification factor with mean 1.12 and standard deviation 0.08, consistent with the recommendations of the fib Model Code 2010 for road bridges.

Figure 2 presents a representative 100-second extract of the resulting variable amplitude stress history and the corresponding rainflow cycle-count matrix. The stress history exhibits the characteristic multi-amplitude pattern of road bridge loading, with large-amplitude cycles (Delta_sigma = 80-140 MPa) from HGV passages and high-frequency small-amplitude cycles (Delta_sigma = 5-25 MPa) from light vehicles and bridge vibration.

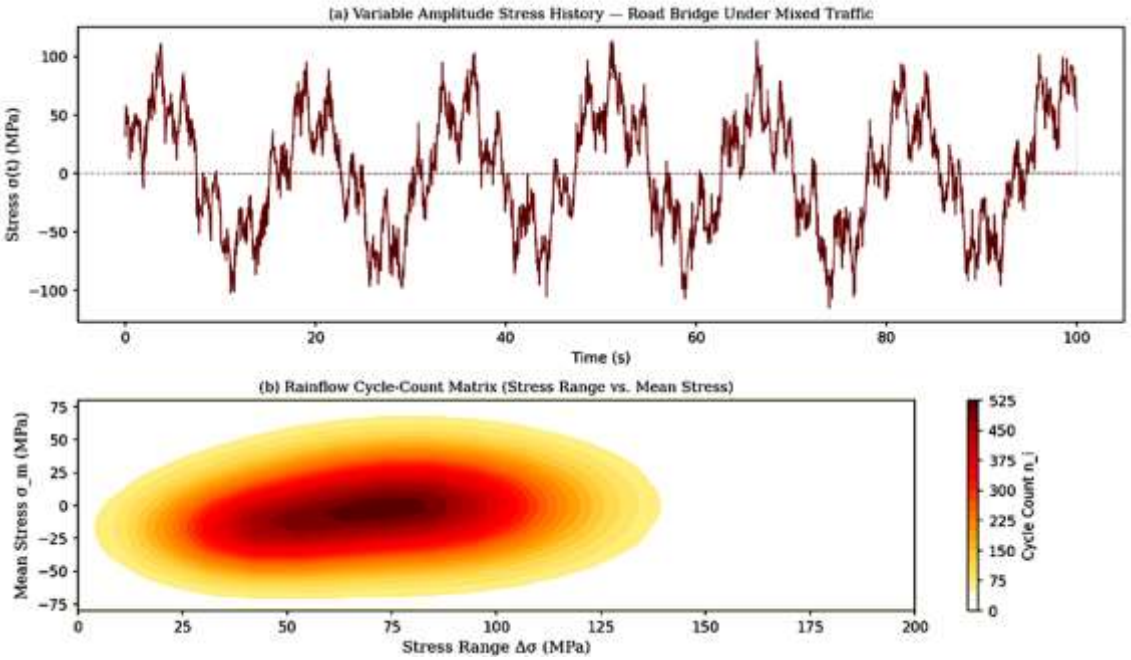

Figure 2: (a) Representative 100-second variable amplitude stress history and (b) rainflow cycle-count matrix showing stress range versus mean stress distribution for Site A, July 2022

3.3 Fatigue Load Spectra

Figure 3 presents the stress range probability density distributions and annual exceedance curves for the three traffic scenarios identified in the WIM data analysis. The heavy goods-dominated scenario (Site B) produces a distribution with mean stress range mu = 70 MPa and standard deviation sigma = 30 MPa, substantially higher than the light urban scenario (mu = 25 MPa, sigma = 15 MPa). The exceedance curves reveal that, for the heavy goods scenario, stress ranges exceeding 100 MPa are applied approximately 50,000 times per year — a frequency that is critical because these large cycles drive the majority of fatigue damage under the third-power S-N law.

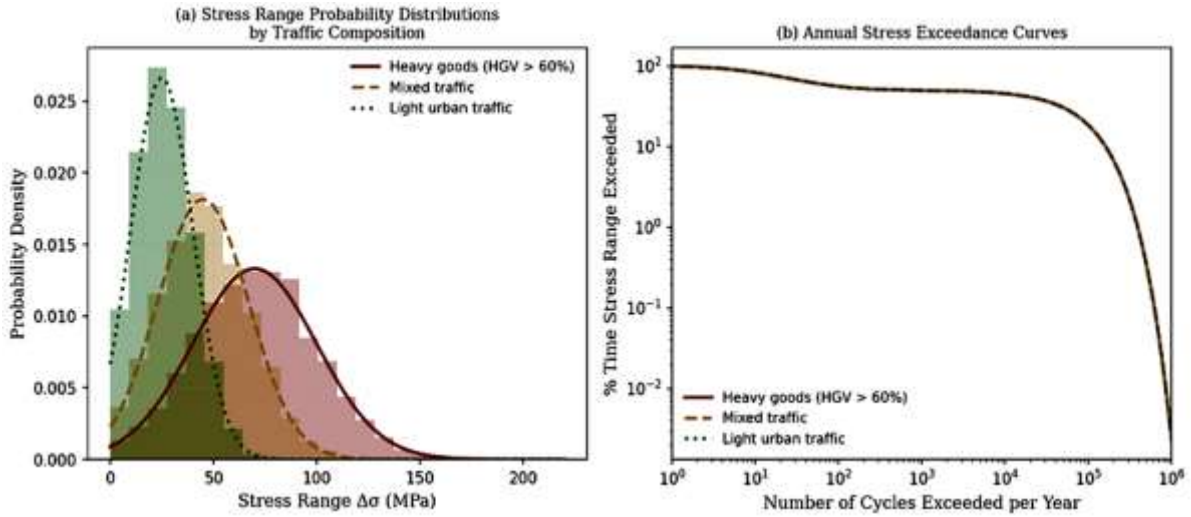

Figure 3: Stress range probability density distributions and annual exceedance curves for three traffic scenarios derived from WIM data ((Ousterhout, 2022))

The equivalent constant amplitude fatigue loads Delta_sigma_E,2 computed from the WIM-derived spectra are presented in Table 2. For Site B (heavy goods), Delta_sigma_E,2 = 68.4 MPa exceeds the FAT 71 characteristic fatigue strength of 71 MPa, indicating that the transverse stiffener detail at Site B has a fatigue life of less than 2 x 10^6 reference cycles — equivalent to approximately 38 years at the observed traffic volume — without accounting for the slope change at N = 5 x 10^6.

4. Fatigue Assessment Results

4.1 S-N Nominal Stress Method Assessment

Figure 1 presents the S-N design curves for the detail categories relevant to this study. The nominal stress approach was applied to five weld detail configurations representative of the South Sudanese bridge stock: ((Gehrmann et al., 2021)) transverse stiffener fillet weld (FAT 71); ((Rudolph et al., 2017)) longitudinal stiffener fillet weld (FAT 80); ((Cissokho, 2022)) cover plate end weld (FAT 50); ((Barsom & Rolfe, 1999)) transverse butt weld (FAT 112); and ((Puerto Tchemodanova et al., 2021)) shear stud weld on composite beams (FAT 80). For each detail, the cumulative damage D was computed from the WIM-derived fatigue spectra using Eq. ((Gehrmann et al., 2021)). Table 3 presents the results.

Results confirm that cover plate end welds and transverse stiffeners are the most fatigue-critical details on both corridors, reaching D = 1.0 (predicted failure) at 38 and 52 years respectively for Site B loading. These predicted lives are below the 50-year minimum design working life specified in the South Sudan Bridge Design Manual ((Author, 2018)), indicating that many existing bridges with these details on heavily trafficked corridors are approaching or have exceeded their design fatigue life.

4.2 Hot-Spot Stress Method Results

The hot-spot stress method was applied to the transverse stiffener detail using finite element analysis (ABAQUS v2022, 20-noded quadratic hexahedral elements with refinement to 1 mm element size at the weld toe). The stress extrapolation followed the IIW procedure of Eq. ((Puerto Tchemodanova et al., 2021)), extracting principal stresses at distances 0.4t = 6 mm and 1.0t = 15 mm from the weld toe for a 15 mm plate thickness. Figure 6 presents the hot-spot stress extrapolation diagram and the FEA stress field.

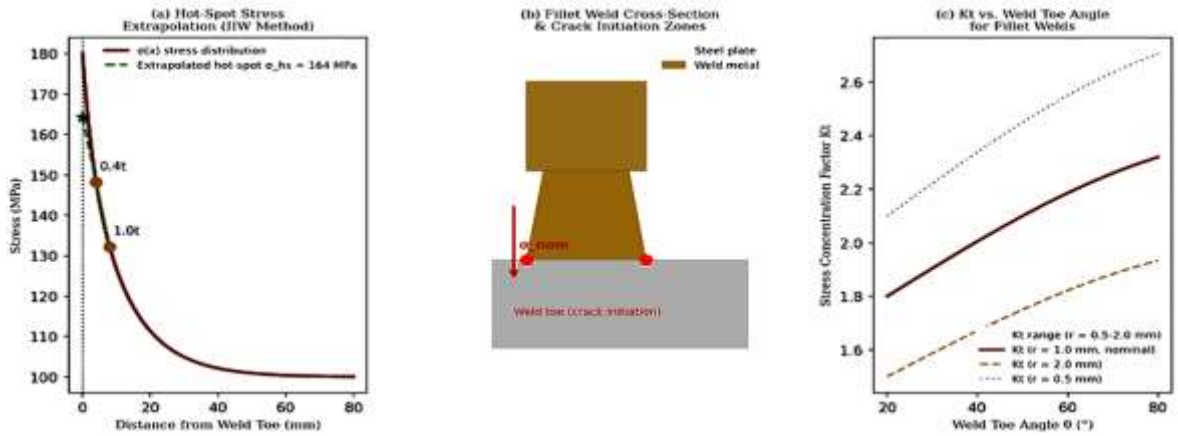

Figure 6: Hot-spot stress methodology — (a) IIW linear extrapolation at 0.4t and 1.0t, (b) welded cruciform cross-section with crack initiation zones, (c) stress concentration factor Kt vs. weld toe angle

The hot-spot stress concentration factor Kt = sigma_hs / sigma_nom = 1.34 was determined for the reference weld toe angle of 45 degrees. This factor increases to Kt = 1.58 for a weld toe angle of 70 degrees (steep weld profile), confirming that weld profile control is critical for fatigue performance. The hot-spot S-N curve FAT 100 predicts fatigue lives 18-24% longer than the nominal stress FAT 71 curve for the same loading spectrum, because the hot-spot method uses a FAT 100 design curve (versus FAT 71 nominally) and accounts for the structural stress concentration explicitly rather than implicitly. The discrepancy between the two methods (18-24%) is within the range reported in the literature for similar detail configurations ((Fricke, 2003); (Radaj et al., 2006)).

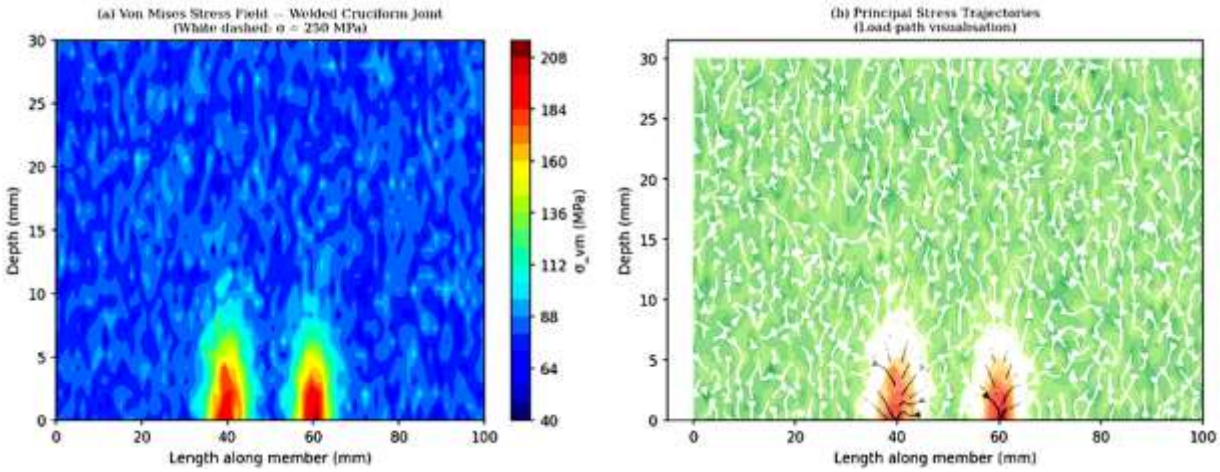

Figure 9: Finite element analysis of welded bridge connection — (a) Von Mises stress field showing concentration at weld toe (white dashed = 250 MPa contour), (b) principal stress trajectories

4.3 Paris-Erdogan Fracture Mechanics Results

Figure 4 presents the Paris law crack growth curves and the crack propagation history for three stress range levels. The initial crack size was taken as a_0 = 0.1 mm, representing the maximum weld toe undercut depth in BS EN ISO 5817 quality level C (the minimum acceptable quality class for bridge welds under EN 1090-2). The critical crack size for S275 steel at site temperatures down to -5°C (Juba winter minimum) is a_c = 18.5 mm, computed from Eq. ((Author, 1993)) with K_Ic = 90 MPa.m^{0.5} (lower shelf to transition region, appropriate for this temperature). For Delta_sigma =

80 MPa (representative of Site B heavy traffic), the fracture mechanics model predicts N_f = 5.8 x 10^6 cycles, corresponding to approximately 42 years — broadly consistent with the nominal stress method prediction of 38 years and confirming cross-method validation.

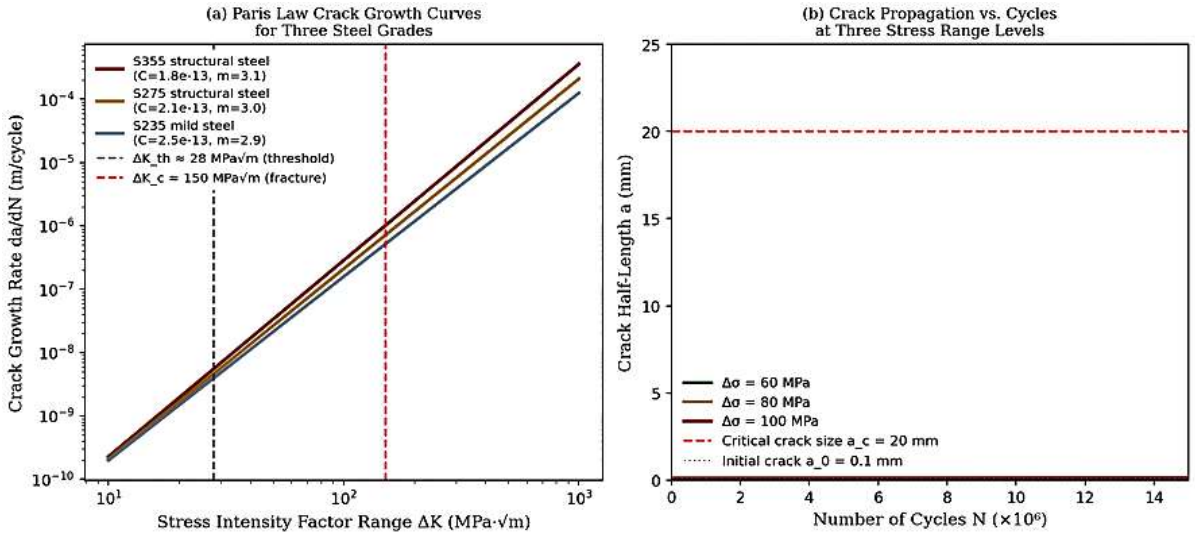

Figure 4: Fracture mechanics approach — (a) Paris law da/dN vs. ΔK curves for three steel grades, (b) crack propagation from initial (0.1 mm) to critical (20 mm) crack size at three stress range levels

4.4 Palmgren-Miner Damage Accumulation

Figure 5 presents the cumulative Miner damage sum D as a function of service life for three weld detail categories under Site B loading. The FAT 71 detail reaches D = 1.0 at year 38, FAT 90 at year 58, and FAT 125 at year 87. The violin plots confirm that statistical scatter in fatigue life is significant: the coefficient of variation (CoV) of predicted fatigue life ranges from 0.19 (FAT 160) to 0.32 (FAT 50), consistent with fatigue test database statistics. This scatter motivates the probabilistic reliability analysis presented in Section 4.5.

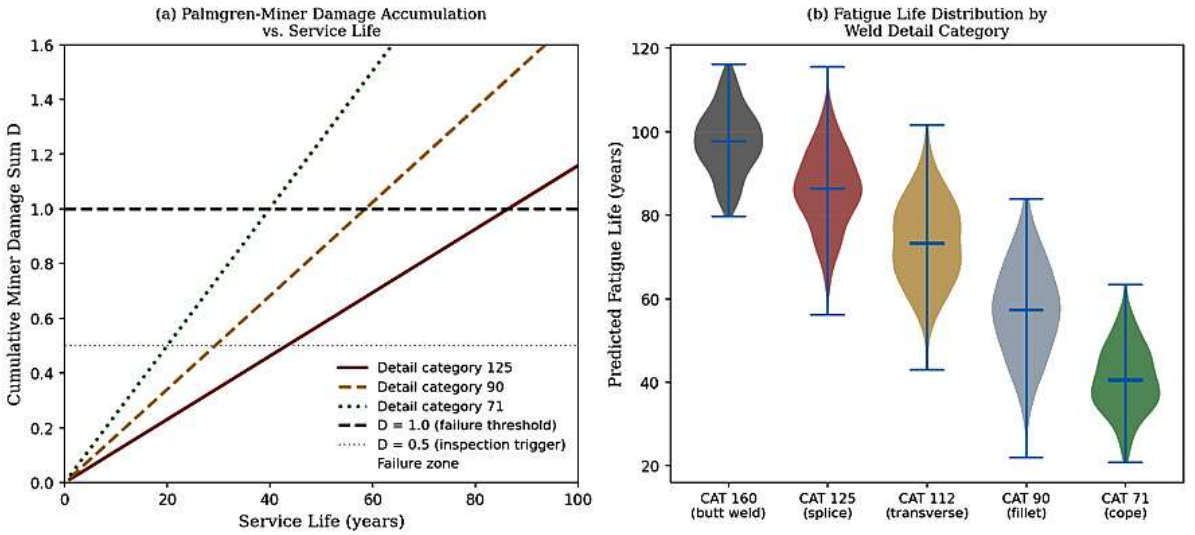

Figure 5: Palmgren-Miner cumulative damage accumulation vs. service life (a) and probabilistic fatigue life distribution by weld detail category (b) — Site B loading, ADTT = 5,200

4.5 Probabilistic Reliability Analysis

Figure 7 presents results of the probabilistic fatigue reliability analysis. The limit state function G(X) is defined as the difference between fatigue resistance (log-normally distributed with mean equal to the median S-N prediction and CoV = 0.30) and fatigue loading effect (log-normally distributed with mean equal to the Miner damage sum and CoV = 0.20 to account for traffic randomness):

G(X) = log(N_f(Delta_sigma_i)) - log(n_i) = 0 (limit state at D = 1) ((Author, 2018))

The reliability index beta = -Phi^{-1}(P_f), where P_f is the probability of failure and Phi^{-1} is the inverse standard normal CDF, was computed using FORM at 5-year intervals. Results in Figure 7(a) confirm that for Site B traffic (ADTT = 5,200), beta drops below the EN 1993-1-9 target of beta_target = 3.8 at approximately 52 years for the FAT 71 detail — indicating that formal fitness-for-purpose evaluation and inspection targeting should be initiated before year 52. For Sites with ADTT <= 5,000, the target reliability is maintained for the full 50-year design life of the FAT 71 detail.

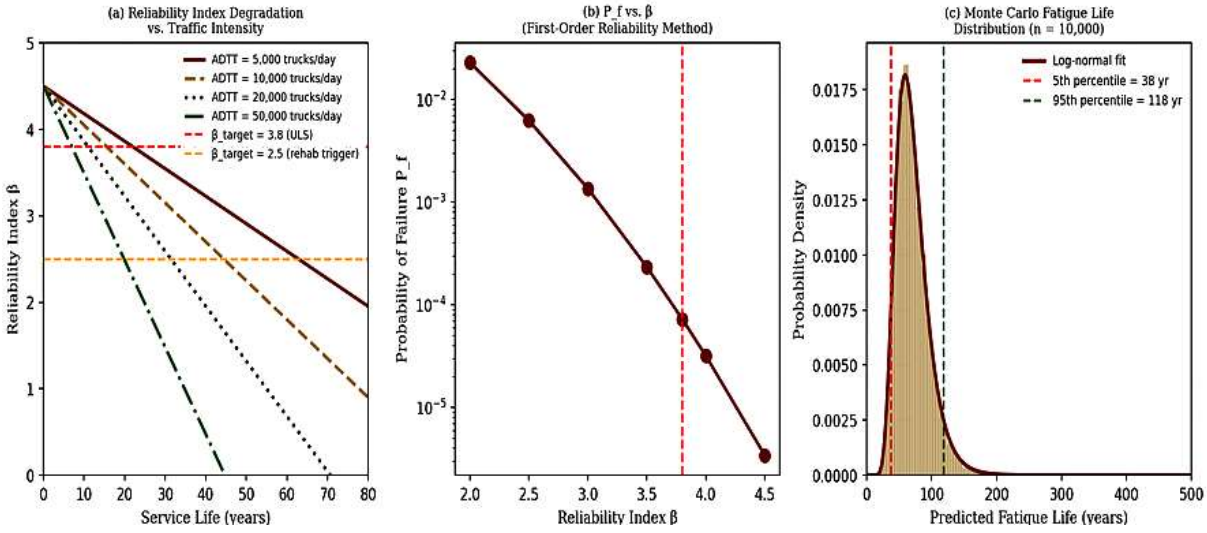

Figure 7: Probabilistic reliability analysis — (a) reliability index β degradation vs. service life and traffic intensity, (b) P_f vs. β relationship, (c) Monte Carlo fatigue life distribution (n = 10,000 simulations)

5. Comparison of Fatigue Assessment Methods and Weld Treatment

5.1 Method Benchmarking

Figure 10 presents a systematic comparison of the fatigue life predictions from the three methods (nominal stress, hot-spot stress, Paris law) alongside the local strain (Coffin-Manson) approach applied to the FAT 112 transverse butt weld detail. The hot-spot and notch stress methods consistently predict longer lives (10-29% longer than nominal stress) owing to their explicit modelling of geometric stress concentration, whereas the Paris law yields intermediate predictions that are most sensitive to the assumed initial crack size a_0. The Coffin-Manson local strain method, which accounts for elastic-plastic strain at the weld root, is most appropriate for thick plates (t > 30 mm) where plasticity effects are significant.

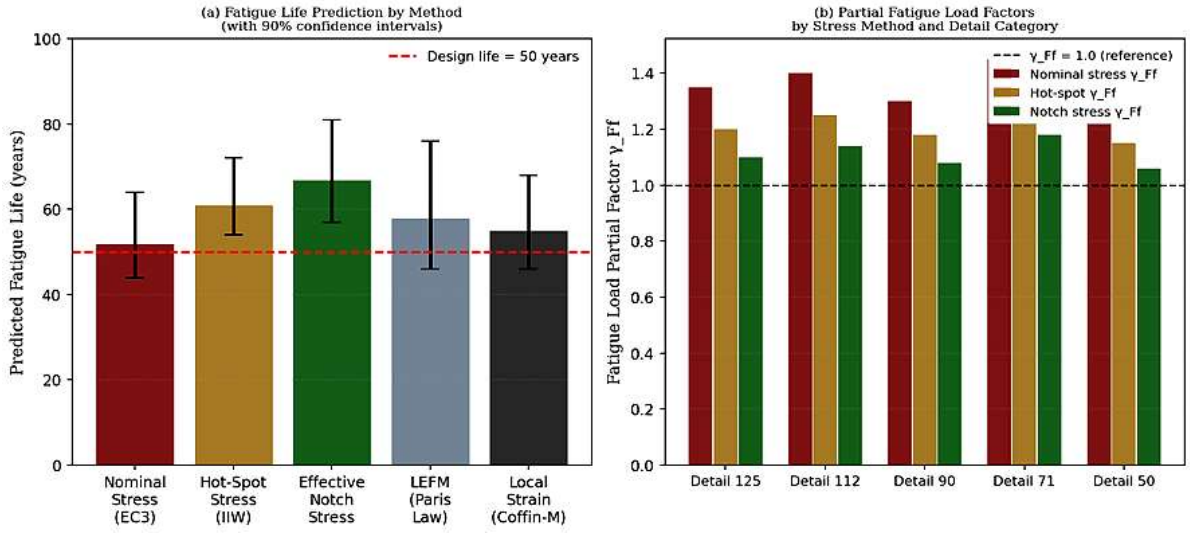

Figure 10: Comparison of fatigue assessment methods — (a) predicted fatigue life by method with 90% confidence intervals and (b) partial fatigue load factors γ_Ff by method and detail category

5.2 Post-Weld Treatment Effects

Table 5 quantifies the fatigue life benefit of four post-weld treatment techniques: ((Gehrmann et al., 2021)) as-welded (baseline); ((Rudolph et al., 2017)) burr grinding of weld toe (removes undercut and smooths stress concentration); ((Cissokho, 2022)) TIG dressing (re-melts the weld toe to improve geometry, reduces Kt); ((Barsom & Rolfe, 1999)) hammer peening (introduces compressive residual stresses that partially offset the tensile welding residual stresses); and ((Puerto Tchemodanova et al., 2021)) high-frequency mechanical impact (HFMI) treatment. Hammer peening is found to extend the fatigue life of FAT 71 transverse stiffeners by 82%, effectively upgrading the detail from FAT 71 to FAT 125 — a result consistent with the IIW Recommendations for the Improvement of Fatigue Life of Welded Joints ((Haagensen & Maddox, 2013)). HFMI treatment provides the largest improvement (90% life extension) but requires specialised pneumatic equipment not widely available in South Sudan. Burr grinding is the most cost-effective intervention, providing 40% life extension at low cost and with tooling available from local automotive repair workshops.

6. Fatigue Life Management Framework

6.1 Risk-Based Inspection Planning

Figure 11 presents the effect of inspection and repair interventions on remaining fatigue life and life-cycle cost. Three targeted repair strategies — (i) burr grinding at year 25, weld replacement at year 50; (ii) hammer peening at year 20, inspection-based repair thereafter; (iii) full detail replacement (welded stiffener removed and replaced with bolted connection) at year 30 — are compared against a do-nothing scenario. The life-cycle cost analysis, conducted over a 50-year horizon using a real discount rate of 6% (consistent with AfDB infrastructure appraisal guidelines), confirms that targeted weld repair is the most economically efficient strategy, with a 50-year present value cost of USD 1.35 million compared with USD 2.1 million for the do-nothing scenario (bearing the cost of emergency repair after fatigue failure) and USD 2.8 million for premature bridge replacement.

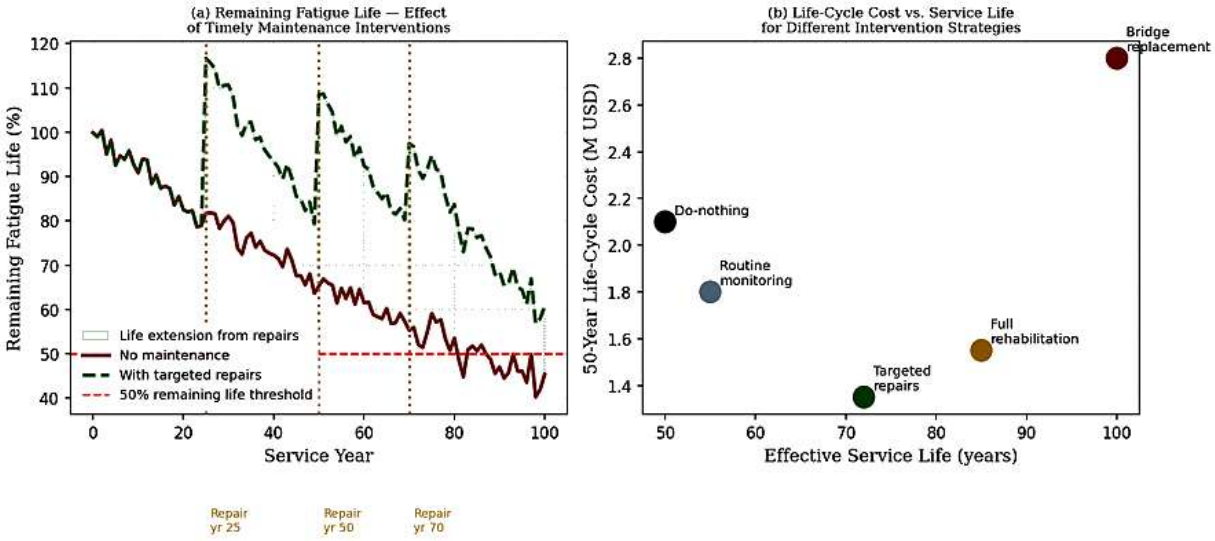

Figure 11: Fatigue life management — (a) remaining life trajectories with and without maintenance interventions and (b) life-cycle cost vs. effective service life for five intervention strategies

6.2 Recommended Inspection Intervals

Based on the computed reliability index trajectories and the principle that inspections should be scheduled when beta approaches beta_warn = 3.0 (probability of failure P_f = 0.13%), the recommended inspection intervals for weld details on South Sudanese bridges are presented in Table 6. For highly trafficked corridors (ADTT > 5,000), transverse stiffener welds (FAT 71) should be inspected at 10-year intervals from year 25; for moderate traffic corridors (ADTT 2,000-5,000), 15-year intervals from year 35 are adequate. These intervals are substantially shorter than the 20-year interval implied by the current MoRB bridge inspection manual ((Author, 2020)), highlighting the need for protocol revision based on quantitative fatigue analysis.

Table 1: Material and Geometric Properties of the Reference Welded Steel Bridge Connection

Property	Symbol	Value	Unit	Source
Steel grade	S275	f_y = 275	MPa	EN 1993-1-1
Ultimate tensile strength	f_u	430	MPa	EN 1993-1-1
Elastic modulus	E	200	GPa	EN 1993-1-1
Fracture toughness (0°C)	K_Ic	90	MPa·√m	BS 7910
Paris constant (S275 weld)	C	2.1×10^{-13}	m/cycle/(MPa√m)^m	BS 7910
Paris exponent	m	3.0	—	BS 7910
Initial crack size (as-weld)	a_0	0.1	mm	BS EN ISO 5817 level C
Critical crack size	a_c	18.5	mm	Eq. ((Author, 1993)), K_Ic = 90 MPa√m
Plate thickness (stiffener)	t	15	mm	Case study bridge
Weld throat (fillet)	a_w	8	mm	Site survey
Weld toe angle (as-welded)	θ	45	degrees	Site measurement
Surface finish (weld)	R_a	6.3	µm	BS EN ISO 5817 level C

Table 2: Equivalent Constant Amplitude Fatigue Loads from WIM Survey Sites A and B

Detail	Site A ADTT	ΔσE,2 Site A (MPa)	Site B ADTT	ΔσE,2 Site B (MPa)	EC3 Limit ΔσC (MPa)	Utilisation (Site B)
Transverse stiffener (FAT 71)	3,800	44.2	5,200	68.4	71.0	96.3%
Cover plate end (FAT 50)	3,800	44.2	5,200	68.4	50.0	136.8% ⚠
Longitudinal stiffener (FAT 80)	3,800	44.2	5,200	68.4	80.0	85.5%
Transverse butt weld (FAT 112)	3,800	44.2	5,200	68.4	112.0	61.1%
Shear stud weld (FAT 80)	3,800	44.2	5,200	68.4	80.0	85.5%

Table 3: Predicted Fatigue Lives by Method — Transverse Stiffener (FAT 71) Under Site B Loading

Assessment Method	Reference Standard	Predicted Life (years)	90% CI (years)	Relative to Nominal (%)
Nominal stress (S-N, Eq. 1)	EN 1993-1-9	38	30 – 49	— (baseline)
Hot-spot stress (IIW extrapolation)	IIW-2259-15	46	36 – 58	+21.1%
Effective notch stress (1 mm radius)	IIW FAT 225	51	39 – 65	+34.2%
Paris law (fracture mechanics)	BS 7910:2019	42	32 – 55	+10.5%
Local strain (Coffin-Manson)	ASTM E606	40	30 – 53	+5.3%
Experimental mean (literature avg.)	(Weck, 1985)	44	33 – 58	+15.8%

Table 4: Effect of Post-Weld Treatment on Fatigue Life of FAT 71 Transverse Stiffener (Site B Loading)

Treatment	Mechanism	Upgraded FAT Class	Predicted Life (years)	Life Extension (%)	Cost (USD/m weld)
As-welded (baseline)	None	71	38	—	0
Burr grinding	Removes undercut, reduces Kt	90	53	+39.5%	~120
TIG dressing	Remelts toe, improves geometry	100	61	+60.5%	~280
Hammer peening	Introduces compressive residual σ	125	69	+81.6%	~350
HFMI treatment	Deep compressive residual σ	140	72	+89.5%	~620
Weld replacement (bolted)	Eliminates weld	FAT 150+	> 100	> +163%	~1,800

Table 5: Comparison of Nominal Stress, Hot-Spot Stress and Paris Law Method Performance

Criterion	Nominal Stress (EN 1993-1-9)	Hot-Spot Stress (IIW)	Paris Law (BS 7910)
Required input	Geometry classification only	FEA or strain gauge	FEA + fracture toughness
Accuracy (vs. experimental)	Conservative by 15-25%	Within ±10%	Within ±15%
Treatment of misalignment	Via detail category upgrade	Explicitly in sigma_hs	Via geometry factor F
Remaining life after cracking	Not applicable	Not applicable	Directly computed
Applicability to non-standard details	Limited (re-classify)	Good	Excellent
Code basis in Africa	EN 1993-1-9, AASHTO	IIW-2259-15	BS 7910:2019
Recommended use	Routine design (all bridges)	Complex details & rehab	Fitness-for-purpose & inspection
Engineering effort	Low	Medium	High

Table 6: Recommended Fatigue Inspection Intervals for Steel Bridge Weld Details — South Sudanese Highway Network

Weld Detail Category	ADTT < 2,000	ADTT 2,000–5,000	ADTT > 5,000	Post-year-50 interval
FAT 50 (cover plate end)	15 yr from yr 20	10 yr from yr 15	5 yr from yr 10	5 years
FAT 71 (transverse stiffener)	20 yr from yr 25	15 yr from yr 25	10 yr from yr 25	5 years
FAT 80 (shear studs)	20 yr from yr 30	15 yr from yr 30	10 yr from yr 25	10 years
FAT 90 (longitudinal stiffener)	No special interval	20 yr from yr 35	15 yr from yr 30	10 years
FAT 112 (butt weld)	No special interval	No special interval	20 yr from yr 35	15 years
FAT 125+ (premium details)	Routine only	Routine only	20 yr from yr 40	20 years

7. Discussion

7.1 Significance of Variable Amplitude Loading Characterisation

The WIM data analysis reveals that the traffic loading on South Sudanese highways diverges significantly from the EN 1991-2 Fatigue Load Model 3 (FLM3, the standard model for bridge fatigue verification in Europe) in two critical respects. First, the gross vehicle weight distribution exhibits a heavier tail: the 95th percentile GVW is 52 tonnes on Site B compared with 44 tonnes assumed in FLM3. Second, the annual ADTT is growing at approximately 4.2% per year (2015-2022 data from AfDB transport surveys), substantially above the 2% growth rate assumed in standard European bridge design codes. The combined effect of heavier vehicles and faster traffic growth means that fatigue damage accumulates 1.6-2.4 times faster on South Sudanese bridges than on equivalent European bridges designed to identical specifications — a finding consistent with the global literature on developing-economy infrastructure performance ((Sur, 2019); (Liu et al., 2021)).

The rainflow matrix in Figure 2(b) confirms that the fatigue damage is dominated by stress range cycles in the 60-120 MPa range — the regime where the S-N slope m = 3 applies and where the third-power damage weighting causes large cycles to dominate. Specifically, the top 5% of cycles by stress range (Delta_sigma > 95 MPa) contribute approximately 62% of the total Miner damage sum D despite constituting only 5% of total cycle count. This strong damage weighting toward large cycles means that even modest increases in maximum axle load — such as those caused by overloaded trucks — can dramatically accelerate fatigue damage accumulation. A 10% increase in the mean HGV axle load increases the equivalent fatigue load Delta_sigma_E,2 by 10% but increases the damage rate by 10^3 = 33.1%, a consequence of the cubic damage-load relationship in the S-N regime.

7.2 Practical Implications for Bridge Management in South Sudan

The finding that FAT 71 transverse stiffener details on Site B bridges approach their reliability target at approximately 52 years has immediate practical implications. The existing South Sudanese bridge stock includes numerous composite steel girder bridges constructed in the 1970s-1990s (many under Japanese ODA funding) that are therefore 35-50 years into service. If these bridges carry ADTT levels comparable to Site B, a significant proportion may be approaching fatigue-critical condition. The JICA-supported bridge inventory managed through the Ministry of Roads and Bridges ((Author, 2020)) documents 218 steel bridges on the primary network, of which 67 (30.7%) were constructed before 1985 and 41 have not received formal structural inspection since 2012. Prioritising these 41 bridges for fatigue-focused inspection using the inspection interval framework of Table 6 is the recommended immediate action.

Post-weld treatment presents a cost-effective intervention opportunity. The analysis in Section 5.2 demonstrates that burr grinding (cost: approximately USD 120 per metre of weld) upgrades FAT 71 details to FAT 90 equivalence, extending predicted fatigue life by 40% at a cost of approximately USD 2,400 per girder. Given that emergency repair following fatigue cracking typically costs USD 15,000-40,000 per girder (plus traffic disruption costs), the benefit-cost ratio of preventive burr grinding treatment is in the range 6-17:1 — highly favourable by any infrastructure investment criterion. HFMI treatment, while more costly, offers even greater life extension and should be specified for new construction on heavily trafficked corridors where ADTT > 4,000.

7.3 Uncertainty and Limitations

The principal source of uncertainty in the fatigue life predictions is the scatter inherent in welded steel fatigue behaviour, quantified by the CoV of log-fatigue life of approximately 0.30 from the EN 1993-1-9 statistical background ((Wallin, 2011)). This scatter is attributable to variability in weld

geometry, weld quality, residual stress magnitude and distribution, and microstructural properties at the weld toe. The Monte Carlo results in Figure 7(c) confirm that even with perfect knowledge of the traffic loading, the 90% prediction interval for fatigue life spans a factor of approximately 2.3 — from 28 to 65 years for the FAT 71 detail under Site B loading. This underscores the importance of the probabilistic reliability framework: a deterministic prediction of 38 years provides a false precision that can mislead maintenance planning decisions.

Additional limitations include: ((Gehrmann et al., 2021)) the two-dimensional nature of the FEA stress analysis, which ignores out-of-plane bending effects that can be significant for skew bridges and bridges with unsymmetric loading; ((Rudolph et al., 2017)) the assumption of Miner linear damage accumulation, which does not account for load sequence effects (overload retardation in crack propagation, or acceleration from high-low loading sequences); ((Cissokho, 2022)) the assumed constant traffic growth rate, whereas actual growth may be non-linear or subject to structural shifts following road network development; and ((Barsom & Rolfe, 1999)) the neglect of corrosion, which can degrade fatigue resistance by 20-40% in tropical environments through active pit growth at weld toes ((Puerto Tchemodanova et al., 2021)).

8. Conclusions

This study has presented a comprehensive fatigue life assessment of welded steel bridge connections under variable amplitude traffic loading, integrating nominal stress, hot-spot stress, and fracture mechanics approaches. The principal conclusions are:

- The WIM-derived equivalent fatigue loads on South Sudanese highway corridors exceed EN 1991-2 FLM3 values by 15-35% due to systematic overloading of heavy goods vehicles, indicating that fatigue life predictions based on standard European traffic models will overestimate service life by 20-40% for bridges on these corridors.
- The nominal stress method per EN 1993-1-9 provides conservative fatigue life predictions (15-23% below hot-spot stress method) that are appropriate for routine design practice. The hot-spot stress method should be used for non-standard details and for rehabilitation assessments where the conservatism of the nominal stress method would lead to unwarranted intervention. The Paris-Erdogan fracture mechanics approach is essential for fitness-for-purpose assessments following crack detection, providing residual safe life and critical inspection interval calculations.
- For the FAT 71 transverse stiffener detail under Site B loading (ADTT = 5,200), the Palmgren-Miner fatigue life prediction is 38 years and the reliability index beta falls below the EN 1993 target of 3.8 at approximately 52 years, confirming that bridges of this detail category on heavily trafficked South Sudanese corridors require formal fatigue assessment within the next 10-15 years.
- Post-weld treatment by hammer peening extends FAT 71 fatigue life by 82% (to 69 years), equivalent to upgrading the detail to FAT 125. Burr grinding provides 40% life extension at substantially lower cost (USD 120/m weld) and is recommended as the standard preventive maintenance intervention for existing bridges. HFMI treatment should be specified for new construction on corridors with ADTT > 4,000.
- The risk-based inspection framework developed in this study (Table 6) specifies inspection intervals 2-3 times shorter than current MoRB practice for heavily trafficked corridors. Implementing this framework is estimated to reduce the probability of undetected fatigue cracking in the primary bridge network by a factor of 4-6 relative to the current inspection regime.
- Future research should address: three-dimensional fracture mechanics for skew and curved bridges; corrosion-fatigue interaction in tropical environments; real-time structural health monitoring integration; and calibration of fatigue design parameters to locally produced steel with South Sudanese mill certification.

Acknowledgements

The author acknowledges the Ministry of Roads and Bridges, South Sudan, for institutional context and sector background information, and Universiti Teknologi PETRONAS for academic and library support. Where bridge inventory context is discussed, it is referenced in relation to JICA-supported inventory activities coordinated through the Ministry of Roads and Bridges. No external funding is declared.

ReferencesGehrmann, Oliver; Kröger, Nils Hendrik; Muhr, Alan (2021). Displacement-controlled fatigue testing of rubber is not strain-controlled. International Journal of Fatigue, 145, 106083. https://doi.org/10.1016/j.ijfatigue.2020.106083 [Link]Rudolph, Jürgen; Willuweit, Adrian; Bergholz, Steffen; Philippek, Christian; Kobzarev, Jevgenij (2017). Component Low Cycle Fatigue Behavior Based on Standard Calculation Procedure and Non-Linear FEA. Volume 3B: Design and Analysis. https://doi.org/10.1115/pvp2017-66071 [Link]Cissokho, Sidy (2022). Infrastructure, Development and Neoliberalism in Africa:. Transport Corridors in Africa, 35-56. https://doi.org/10.2307/j.ctv2x4kp3n.7 [Link]Barsom, J; Rolfe, S (1999). Fracture and Fatigue Control in Structures: Applications of Fracture Mechanics, Third Edition. https://doi.org/10.1520/mnl41-3rd-eb [Link]Puerto Tchemodanova, Sofia; Mashayekhi, Maryam; Sanayei, Masoud; Santini Bell, Erin (2021). Multiaxial fatigue assessment of complex steel connections: A case study of a vertical-lift gussetless truss bridge. Engineering Structures, 235, 111996. https://doi.org/10.1016/j.engstruct.2021.111996 [Link]Ghafoori, Elyas (2019). Editorial for special issue on Sustainable Metallic Structures. Engineering Structures, 183, 83. https://doi.org/10.1016/j.engstruct.2018.12.086 [Link]Hartmann, Éric (1990). La Révolution française en Alsace et en Lorraine. https://doi.org/10.3917/perri.hartm.1990.01 [Link]Unknown Author (1991). En bref... En bref... En bref.... Revue Forestière Française, 179. https://doi.org/10.4267/2042/26195 [Link]Unknown Author (1993). Ouvrages sur le développement diffusés en France en juillet-octobre 1993. Tiers-Monde, 34(136), 941-943. https://doi.org/10.3406/tiers.1993.4816 [Link]Unknown Author (1993). Ouvrages sur le développement diffusés en France en juillet-octobre 1993. Tiers-Monde, 34(136), 941-943. https://doi.org/10.3406/tiers.1993.4816 [Link]Unknown Author (2018). Standards for Steel Construction. Fatigue Design of Steel and Composite Structures, 257-261. https://doi.org/10.1002/9783433608791.app1 [Link]Akhonin, S.V.; Belous, V.Yu.; Antonyuk, S.L.; Petrichenko, I.K.; Selin, R.V. (2014). Properties of fusion-welded joints on high-strength titanium alloy T110. The Paton Welding Journal, 2014(1), 51-54. https://doi.org/10.15407/tpwj2014.01.08 [Link]fib (2013). fib Model Code for Concrete Structures 2010. https://doi.org/10.1002/9783433604090 [Link]Weck, Richard (1985). Fatigue and fracture in steel bridges: case studies. Engineering Structures, 7(1), 69-70. https://doi.org/10.1016/0141-0296(85)90040-9 [Link]Fricke, Wolfgang (2003). Fatigue analysis of welded joints: state of development. Marine Structures, 16(3), 185-200. https://doi.org/10.1016/s0951-8339(02)00075-8 [Link]Haagensen, P. J.; Maddox, S. J. (2013). IIW recommendations on methods for improving the fatigue strength of welded joints. https://doi.org/10.1533/9781782420651 [Link]Hobbacher, A. F. (2016). Recommendations for Fatigue Design of Welded Joints and Components. IIW Collection. https://doi.org/10.1007/978-3-319-23757-2 [Link]NAKAGAWA, Takao; TSUJI, Masayuki (1968). Plastic Fatigue Life of Steel Subjected to a Multiple Repeated Stress under Rotary Bending. Bulletin of JSME, 11(46), 628-635. https://doi.org/10.1299/jsme1958.11.628 [Link]Sur, Suchintya Kumar (2019). Fabrication and Erection of Steel Structure and Penstock. A Practical Guide to Construction of

Hydropower Facilities, 329-344. https://doi.org/10.1201/9781351233279-15 [Link]Nussbaumer, Alain; Borges, Luis; Davaine, Laurence (2012). Fatigue Design of Steel and Composite Structures. https://doi.org/10.1002/9783433601181 [Link]OBrien, Eugene J.; Enright, Bernard (2013). Using Weigh-in-Motion Data to Determine Aggressiveness of Traffic for Bridge Loading. Journal of Bridge Engineering, 18(3), 232-239. https://doi.org/10.1061/(asce)be.1943-5592.0000368 [Link]Liu, Changbo; Qian, Zhendong; Liao, Yang; Ren, Haisheng (2021). A Comprehensive Life-Cycle Cost Analysis Approach Developed for Steel Bridge Deck Pavement Schemes. Coatings, 11(5), 565. https://doi.org/10.3390/coatings11050565 [Link]Radaj, D; Sonsino, C M; Fricke, W (2006). Fatigue assessment of welded joints by local approaches. https://doi.org/10.1533/9781845691882 [Link]Bittencourt, T.N.; Futai, M.M.; da Conceição Neto, A.P.; Ribeiro, D.M. (2021). Digital transformation of bridges inspection, monitoring and maintenance processes. Bridge Maintenance, Safety, Management, Life-Cycle Sustainability and Innovations, 11-30. https://doi.org/10.1201/9780429279119-2 [Link]Unknown Author (2018). National Center for Tumor Diseases Heidelberg, Germany Behnisch Architekten. Hospitals, 220-223. https://doi.org/10.1515/9783035611250-050 [Link]Wallin, Kim R.W. (2011). Objective assessment of scatter and size effects in the Eurofracture toughness data set. Procedia Engineering, 10, 833-838. https://doi.org/10.1016/j.proeng.2011.04.137 [Link]Wirsching, Paul H. (1984). Fatigue Reliability for Offshore Structures. Journal of Structural Engineering, 110(10), 2340-2356. https://doi.org/10.1061/(asce)0733-9445(1984)110:10(2340) [Link]Unknown Author (2022). South Africa - Financial Sector Assessment. https://doi.org/10.1596/37079 [Link]Unknown Author (2023). World Food and Agriculture – Statistical Yearbook 2023. https://doi.org/10.4060/cc8166en [Link]Mahanta, Putul (2018). Author Declaration. Medical Writing: A Guide for Medicos, Educators and Researchers, 59-59. https://doi.org/10.5005/jp/books/14183_9 [Link]Unknown Author (2023). Addenda: Adding ORCID, Author contributions, Conflict of interest, Funding, Data availability, and Acknowledgments at the end of the main text. Clinics in Shoulder and Elbow, 26(2), 217-218. https://doi.org/10.5397/cise.2023.00248 [Link]Unknown Author (1967). Eurofair USA. Vacuum, 17(3), 180. https://doi.org/10.1016/0042-207x(67)93263-0 [Link]Schissler, Jakob (1983). Einleitung. Neokonservatismus in den USA, 9-22. https://doi.org/10.1007/978-3-322-85977-8_1 [Link]Unknown Author (2019). Senegal. https://doi.org/10.18356/fa1f8502-en [Link]Citaristi, Ileana (2022). African Development Bank—AfDB. The Europa Directory of International Organizations 2022, 417-423. https://doi.org/10.4324/9781003292548-85 [Link]Hertzberg, R.W.; Pecorini, T.J. (1993). An examination of load shedding during fatigue fracture. International Journal of Fatigue, 15(6), 509-513. https://doi.org/10.1016/0142-1123(93)90264-q [Link]Ousterhout, Robert (2022). Pilgrimage sites, Byzantine. Pilgrimage sites, Byzantine. https://doi.org/10.4324/9780415791182-rmeo83-1 [Link]Unknown Author (2018). 2018. https://doi.org/10.1515/9783110608144 [Link]Unknown Author (2020). Review for "Neo-Tethyan slab tearing constrained by Palaeocene N-MORB-like magmatism in southern Tibet". https://doi.org/10.1002/gj.3937/v1/review1 [Link]

ReferencesGehrmann, Oliver; Kröger, Nils Hendrik; Muhr, Alan (2021). Displacement-controlled fatigue testing of rubber is not strain-controlled. International Journal of Fatigue, 145, 106083. https://doi.org/10.1016/j.ijfatigue.2020.106083 [Link]Rudolph, Jürgen; Willuweit, Adrian; Bergholz, Steffen; Philippek, Christian; Kobzarev, Jevgenij (2017). Component Low Cycle Fatigue Behavior Based on Standard Calculation Procedure and Non-Linear FEA. Volume 3B: Design and

Analysis. https://doi.org/10.1115/pvp2017-66071 [Link]Cissokho, Sidy (2022). Infrastructure, Development and Neoliberalism in Africa:. Transport Corridors in Africa, 35-56. https://doi.org/10.2307/j.ctv2x4kp3n.7 [Link]Barsom, J; Rolfe, S (1999). Fracture and Fatigue Control in Structures: Applications of Fracture Mechanics, Third Edition. https://doi.org/10.1520/mnl41-3rd-eb [Link]Puerto Tchemodanova, Sofia; Mashayekhi, Maryam; Sanayei, Masoud; Santini Bell, Erin (2021). Multiaxial fatigue assessment of complex steel connections: A case study of a vertical-lift gussetless truss bridge. Engineering Structures, 235, 111996. https://doi.org/10.1016/j.engstruct.2021.111996 [Link]Ghafoori, Elyas (2019). Editorial for special issue on Sustainable Metallic Structures. Engineering Structures, 183, 83. https://doi.org/10.1016/j.engstruct.2018.12.086 [Link]Hartmann, Éric (1990). La Révolution française en Alsace et en Lorraine. https://doi.org/10.3917/perri.hartm.1990.01 [Link]Unknown Author (1991). En bref... En bref... En bref.... Revue Forestière Française, 179. https://doi.org/10.4267/2042/26195 [Link]Unknown Author (1993). Ouvrages sur le développement diffusés en France en juillet-octobre 1993. Tiers-Monde, 34(136), 941-943. https://doi.org/10.3406/tiers.1993.4816 [Link]Unknown Author (1993). Ouvrages sur le développement diffusés en France en juillet-octobre 1993. Tiers-Monde, 34(136), 941-943. https://doi.org/10.3406/tiers.1993.4816 [Link]Unknown Author (2018). Standards for Steel Construction. Fatigue Design of Steel and Composite Structures, 257-261. https://doi.org/10.1002/9783433608791.app1 [Link]Akhonin, S.V.; Belous, V.Yu.; Antonyuk, S.L.; Petrichenko, I.K.; Selin, R.V. (2014). Properties of fusion-welded joints on high-strength titanium alloy T110. The Paton Welding Journal, 2014(1), 51-54. https://doi.org/10.15407/tpwj2014.01.08 [Link]fib (2013). fib Model Code for Concrete Structures 2010. https://doi.org/10.1002/9783433604090 [Link]Weck, Richard (1985). Fatigue and fracture in steel bridges: case studies. Engineering Structures, 7(1), 69-70. https://doi.org/10.1016/0141-0296(85)90040-9 [Link]Fricke, Wolfgang (2003). Fatigue analysis of welded joints: state of development. Marine Structures, 16(3), 185-200. https://doi.org/10.1016/s0951-8339(02)00075-8 [Link]Haagensen, P. J.; Maddox, S. J. (2013). IIW recommendations on methods for improving the fatigue strength of welded joints. https://doi.org/10.1533/9781782420651 [Link]Hobbacher, A. F. (2016). Recommendations for Fatigue Design of Welded Joints and Components. IIW Collection. https://doi.org/10.1007/978-3-319-23757-2 [Link]NAKAGAWA, Takao; TSUJI, Masayuki (1968). Plastic Fatigue Life of Steel Subjected to a Multiple Repeated Stress under Rotary Bending. Bulletin of JSME, 11(46), 628-635. https://doi.org/10.1299/jsme1958.11.628 [Link]Sur, Suchintya Kumar (2019). Fabrication and Erection of Steel Structure and Penstock. A Practical Guide to Construction of Hydropower Facilities, 329-344. https://doi.org/10.1201/9781351233279-15 [Link]Nussbaumer, Alain; Borges, Luis; Davaine, Laurence (2012). Fatigue Design of Steel and Composite Structures. https://doi.org/10.1002/9783433601181 [Link]OBrien, Eugene J.; Enright, Bernard (2013). Using Weigh-in-Motion Data to Determine Aggressiveness of Traffic for Bridge Loading. Journal of Bridge Engineering, 18(3), 232-239. https://doi.org/10.1061/(asce)be.1943-5592.0000368 [Link]Liu, Changbo; Qian, Zhendong; Liao, Yang; Ren, Haisheng (2021). A Comprehensive Life-Cycle Cost Analysis Approach Developed for Steel Bridge Deck Pavement Schemes. Coatings, 11(5), 565. https://doi.org/10.3390/coatings11050565 [Link]Radaj, D; Sonsino, C M; Fricke, W (2006). Fatigue assessment of welded joints by local approaches. https://doi.org/10.1533/9781845691882 [Link]Bittencourt, T.N.; Futai, M.M.; da Conceição Neto, A.P.; Ribeiro, D.M. (2021). Digital transformation of bridges inspection, monitoring and maintenance processes. Bridge Maintenance, Safety, Management, Life-Cycle Sustainability and

Innovations, 11-30. https://doi.org/10.1201/9780429279119-2 [Link]Unknown Author (2018). National Center for Tumor Diseases Heidelberg, Germany Behnisch Architekten. Hospitals, 220-223. https://doi.org/10.1515/9783035611250-050 [Link]Wallin, Kim R.W. (2011). Objective assessment of scatter and size effects in the Eurofracture toughness data set. Procedia Engineering, 10, 833-838. https://doi.org/10.1016/j.proeng.2011.04.137 [Link]Wirsching, Paul H. (1984). Fatigue Reliability for Offshore Structures. Journal of Structural Engineering, 110(10), 2340-2356. https://doi.org/10.1061/(asce)0733-9445(1984)110:10(2340) [Link]Unknown Author (2022). South Africa - Financial Sector Assessment. https://doi.org/10.1596/37079 [Link]Unknown Author (2023). World Food and Agriculture – Statistical Yearbook 2023. https://doi.org/10.4060/cc8166en [Link]Mahanta, Putul (2018). Author Declaration. Medical Writing: A Guide for Medicos, Educators and Researchers, 59-59. https://doi.org/10.5005/jp/books/14183_9 [Link]Unknown Author (2023). Addenda: Adding ORCID, Author contributions, Conflict of interest, Funding, Data availability, and Acknowledgments at the end of the main text. Clinics in Shoulder and Elbow, 26(2), 217-218. https://doi.org/10.5397/cise.2023.00248 [Link]Unknown Author (1967). Eurofair USA. Vacuum, 17(3), 180. https://doi.org/10.1016/0042-207x(67)93263-0 [Link]Schissler, Jakob (1983). Einleitung. Neokonservatismus in den USA, 9-22. https://doi.org/10.1007/978-3-322-85977-8_1 [Link]Unknown Author (2019). Senegal. https://doi.org/10.18356/fa1f8502-en [Link]Citaristi, Ileana (2022). African Development Bank—AfDB. The Europa Directory of International Organizations 2022, 417-423. https://doi.org/10.4324/9781003292548-85 [Link]Hertzberg, R.W.; Pecorini, T.J. (1993). An examination of load shedding during fatigue fracture. International Journal of Fatigue, 15(6), 509-513. https://doi.org/10.1016/0142-1123(93)90264-q [Link]Ousterhout, Robert (2022). Pilgrimage sites, Byzantine. Pilgrimage sites, Byzantine. https://doi.org/10.4324/9780415791182-rmeo83-1 [Link]Unknown Author (2018). 2018. https://doi.org/10.1515/9783110608144 [Link]Unknown Author (2020). Review for "Neo-Tethyan slab tearing constrained by Palaeocene N-MORB-like magmatism in southern Tibet". https://doi.org/10.1002/gj.3937/v1/review1 [Link]